

## Resummed lattice QCD equation of state at finite baryon density: strangeness neutrality and beyond

Jana N. Guenther,<sup>a,\*</sup> Szabolcs Borsanyi,<sup>a</sup> Zoltan Fodor,<sup>a,b,c,d,e</sup> Matteo Giordano,<sup>c</sup> Sandor D. Katz,<sup>c,f</sup> Ruben Kara,<sup>a</sup> Paolo Parotto,<sup>b</sup> Attila Pasztor,<sup>c</sup> Claudia Ratti,<sup>g</sup> Kalman K. Szabo<sup>a,d</sup> and Chik Him Wong<sup>a</sup>

<sup>a</sup>Department of Physics, Wuppertal University, Gausstr. 20, D-42119, Wuppertal, Germany

<sup>b</sup>Pennsylvania State University, Department of Physics, University Park, PA 16802, USA

<sup>c</sup>Inst. for Theoretical Physics, ELTE Eötvös Loránd University, Pázmány P. sétány 1/A, H-1117 Budapest, Hungary

<sup>d</sup>Jülich Supercomputing Centre, Forschungszentrum Jülich, D-52425 Jülich, Germany

<sup>e</sup>Physics Department, UCSD, San Diego, CA 92093, USA

<sup>f</sup>MAT-ELTE Theoretical Physics Research Group, Pázmány Péter sétány 1/A, H-1117 Budapest, Hungary

<sup>g</sup>Department of Physics, University of Houston, Houston, TX 77204, USA

E-mail: [jguenther@uni-wuppertal.de](mailto:jguenther@uni-wuppertal.de)

We calculate a resummed equation of state with lattice QCD simulations at imaginary chemical potentials, generalizing the scheme introduced in our previous work to the case of non-zero  $\mu_S$ , and focusing on the line of strangeness neutrality. We present results up to  $\mu_B/T \leq 3.5$  on the strangeness neutral line  $\langle S \rangle = 0$  in the temperature range  $130 \text{ MeV} \leq T \leq 280 \text{ MeV}$ . We also extrapolate the finite baryon density equation of state to small non-zero values of the strangeness-to-baryon ratio  $R = \langle S \rangle / \langle B \rangle$ . We perform a continuum extrapolation using lattice simulations of the 4stout-improved staggered action with 8, 10, 12 and 16 time slices. Finally we test the resummation scheme in a small volume by comparison with direct simulations.

*The 39th International Symposium on Lattice Field Theory,  
8th-13th August, 2022,  
Rheinische Friedrich-Wilhelms-Universität Bonn, Bonn, Germany*

\*Speaker

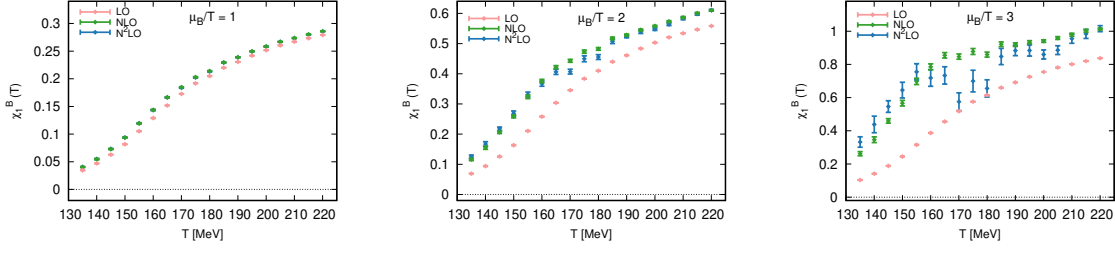


**Figure 1:** (Ref. [12, 14]) The extrapolation of  $\chi_1^B$  to finite baryon chemical potential on a lattice of size  $48^3 \times 12$ .

## 1. Analytic continuation and the equation of state

The equation of state at vanishing baryon chemical potential  $\mu_B$  is known from lattice QCD simulations in the continuum limit (Refs. [1–3]) up to high enough temperatures to be matched to perturbative results (Refs. [4–6]).

To extend the equation of state to finite chemical potentials it is common to use a Taylor expansion in the chemical potentials for the pressure:

$$\hat{p} = \frac{P}{T^4}(T, \hat{\mu}_B, \hat{\mu}_S) = \sum_{ijk} \frac{1}{i!j!} \chi_{i,j}^{BS}(T) \hat{\mu}_B^i \hat{\mu}_S^j, \quad (1)$$

with

$$\chi_{ij}^{BS} = \frac{\partial^{i+j} \hat{p}}{\partial^i \hat{\mu}_B \partial^j \hat{\mu}_S} \quad (2)$$

and the dimensionless chemical potentials are  $\hat{\mu}_i = \frac{\mu_i}{T}$ . It is possible to include the charge chemical potential  $\mu_Q$  in the expansion, however in this proceedings  $\mu_Q = 0$  leading to  $\chi_1^Q = 0.5\chi_1^B$ . The influence of tuning this relation to  $\chi_1^Q = 0.4\chi_1^B$  is shown to be small in Ref. [7]. The expansion coefficients  $\chi_{ij}^{BS}$  are interesting lattice observables with a variety of applications. They are known up to the fourth order derivatives in the continuum limit (Refs. [8–11]) and up to 8th order at finite lattice spacing (Refs. [11–13]).

If one computes the Taylor expansion of  $\chi_1^B$  up to the third order and to  $\mu_B/T \gtrsim (2 - 2.5)$  it shows undesirable properties for temperatures slightly above the crossover transition as shown in Figure 1. In Ref. [14] this behavior has been reproduced in a simple toy model for truncation of the Taylor expansion but vanishes for the infinite Taylor series.

## 2. Rescaling and expansion - the analysis

In Ref. [14] we introduced a resummed extrapolation method that avoids the undesired behavior of the equation of state discussed above for the case of  $\mu_S = \mu_Q = 0$ . We now aim to improve this scheme to achieve results which match the overall strangeness neutrality present in heavy ion collision experiments. This means enforcing the conditions  $\mu_Q = 0$  and  $\chi_1^S = 0$ , yielding a relation between  $\mu_S$  and  $\mu_B$ :

$$\frac{d\mu_S}{d\mu_B} = -\frac{\chi_{11}^{BS}}{\chi_2^S}.$$

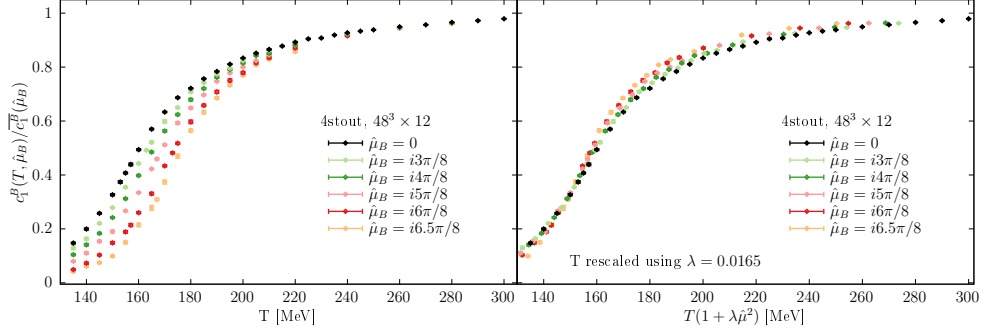


**Figure 2:** (Ref. [7]) Left: The total derivative  $c_1^B$  on the strangeness neutral line from our imaginary chemical potential simulations. The data points at  $\hat{\mu}_B = 0$  show the second derivative  $\frac{d^2 \hat{p}}{d\hat{\mu}_B^2}$ . Right: The same observables, with the temperature rescaled by a factor  $1 + \kappa \hat{\mu}_B^2$ .

On this line, total derivatives with respect to the baryochemical potential read

$$\frac{d}{d\hat{\mu}_B} = \frac{\partial}{\partial \hat{\mu}_B} + \frac{d\hat{\mu}_S}{d\hat{\mu}_B} \frac{\partial}{\partial \hat{\mu}_S} = \frac{\partial}{\partial \hat{\mu}_B} - \frac{\chi_{11}^{BS}}{\chi_2^S} \frac{\partial}{\partial \hat{\mu}_S}.$$

The total derivatives of the pressure on the strangeness neutral line we denote by:

$$c_n^B(T, \hat{\mu}_B) \equiv \left. \frac{d^n \hat{p}(T, \hat{\mu}_B)}{d\hat{\mu}_B^n} \right|_{\substack{\mu_Q=0 \\ \chi_1^S=0}}.$$

We denote the Stefan-Boltzmann limit of those derivatives by  $\overline{c_N^B}(\hat{\mu}_B)$ . In the special case of the net baryon density it does not change compared to the case of  $\mu_S = \mu_Q = 0$ :

$$c_1^B(T, \hat{\mu}_B) = \chi_1^B - \frac{\chi_{11}^{BS}}{\chi_2^S} \underbrace{\chi_1^S}_{=0} = \chi_1^B$$

however, higher order derivatives differ from the  $\chi^{BS}$  and include additional terms which have to be computed.

The resummation scheme introduced in Ref. [14] is based on the approximate shifting of  $c_1^B$  with imaginary  $\mu_B$  for a fixed temperature as shown in figure 2.

The cause of this shifting behavior is not clear. It could suggest an approximate scaling variable in the equation of state. It could be related to the critical scaling in the chiral limit. If the universal contribution to  $c_1^B$  is large, the curves are expected to approximately keep their shape. Furthermore, this observation is consistent with the fits to the observation of constant width of the transition reported in reference [15]. Regardless, the general idea of the resummation method works, even if the shape of the curves is changing. However, the fast convergence is caused by the vanishing of higher order contributions which means, that the shape of the curves is kept.

To further improve the scheme, we need to address the fact that our extrapolation method will fail at high temperatures. To avoid this we introduced a correction by dividing  $c_1^B$  by its Stefan-Boltzmann limit. As can be seen in figure 3 the approximate shift is still there after this correction.

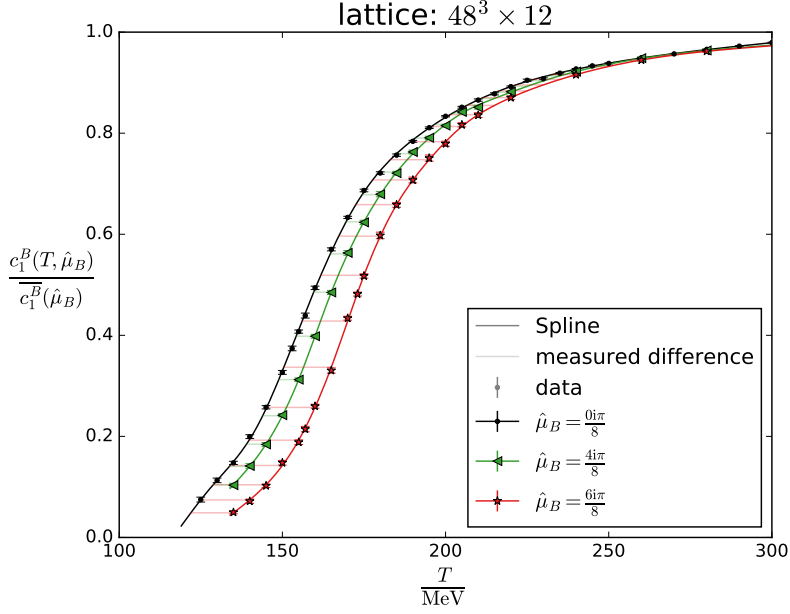


**Figure 3:** (Ref. [7]) Illustration of the measurement of our proxy  $\Pi(T, \hat{\mu}_B, N_\tau) = \frac{T'(T, \hat{\mu}_B, N) - T}{T \hat{\mu}_B}$ .

To make use of it we measure the difference between the curves at  $\hat{\mu}_B = 0$  and at imaginary  $\hat{\mu}_B$  as also illustrated in figure 3. To measure the shift we need to fit a spline function defined at various points through our data points. This allows us to define the proxy:

$$\Pi(T, \hat{\mu}_B, N_\tau) = \frac{T'(T, \hat{\mu}_B, N) - T}{T \hat{\mu}_B}, \quad (3)$$

which we can expand as

$$\Pi(T, \hat{\mu}_B, N_\tau) = \lambda_2^A + \lambda_4^A \hat{\mu}_B^2 + \lambda_6^A \hat{\mu}_B^4 + \frac{1}{N_\tau^2} \left( \alpha^A + \beta^A \hat{\mu}_B^2 + \gamma^A \hat{\mu}_B^4 \right). \quad (4)$$

The  $\lambda_i^A$  coefficients will be used to calculate various quantities for the equation of state.

Our results are based on lattice QCD simulations of 2+1+1 flavours of dynamical quarks with the tree-level Symanzik improved gauge action and four times stout smeared staggered fermions. The simulation is performed on a LCP which is set by pion and kaon mass and at  $\langle n_S \rangle = 0$ . We use four different lattice sizes:  $32^3 \times 8$ ,  $40^3 \times 10$ ,  $48^3 \times 12$  and  $64^3 \times 16$  to estimate the continuum limit. For the imaginary chemical potentials we use the values  $\frac{\mu_B}{T} = i \frac{j\pi}{8}$  with  $j = 0, 3, 4, 5, (5.5), 6$  and 6.5, where the value 5.5 is only available on the  $48^3 \times 12$ -lattice.

To present a comprehensive analysis on the systematic error we use 3 different sets of spline node points at  $\mu_B=0$  and 2 different sets of spline node points at finite imaginary  $\mu_B$ . To set the scale, we use two methods:  $w_0$  or  $f_\pi$  based scale setting. Additionally, we consider 2 different chemical potential ranges in the global fit:  $\hat{\mu}_B \leq 5.5$  or  $\hat{\mu}_B \leq 6.5$ , and we use 2 functions for the chemical potential dependence of the global fit: linear or parabola. We also include or not the coarsest lattice,  $N_\tau = 8$ , in the continuum extrapolation. In total, we perform 96 fits. We weigh every result with a  $Q > 0.01$  uniformly to take into account the quality of the fits.

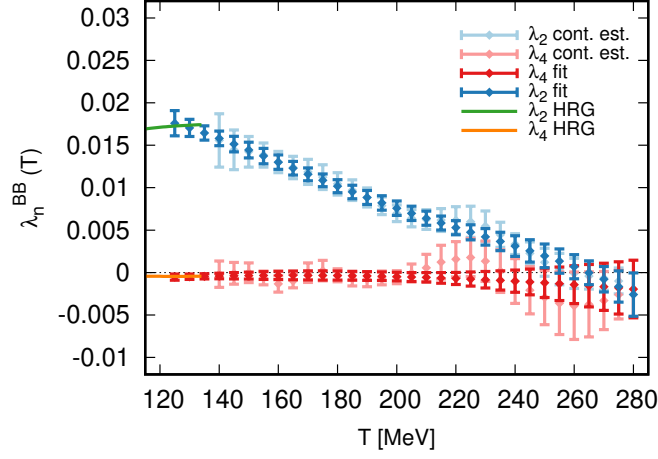


**Figure 4:** (Ref. [7]) The expansion results for the shift proxy of  $c_1^B$  from equation 4.

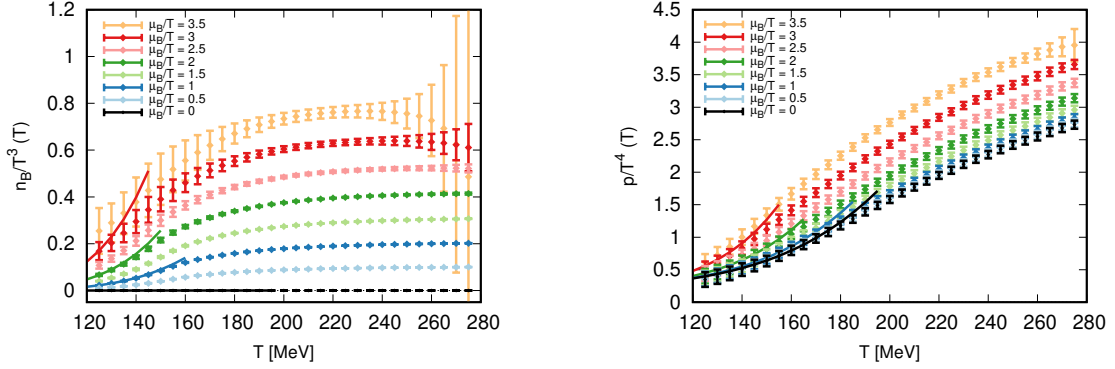


**Figure 5:** (Ref. [7]) Results for  $\frac{n_B}{T^3}$  and  $\frac{p}{T^4}$  at various real chemical potentials along the strangeness neutral line.

The results of this analysis are shown in figure 4. We make a fit to calculate derivatives and constrain it with results from the hadron resonance gas at low temperature, which are also shown in figure 4 and smoothly fit to our data points.

Now we can compute several observables for the equation of state. As an example we show  $\frac{n_B}{T^3}$  and  $\frac{p}{T^4}$  in figure 5.

### 3. Beyond strangeness neutrality

In addition to having results along the strangeness neutral line, we also investigate how the equation of state can be extrapolated to small values of the strangeness density, slightly off the  $\chi_1^S = 0$  line. Therefore we need to repeat the analysis discussed in the previous section for two more observables, that allow us access to the strangeness derivatives as well as the mixed derivatives for  $\hat{\mu}_B$  and  $\hat{\mu}_S$ . We are using the quantities  $\chi_2^S$  and  $\frac{\mu_S}{\mu_B}$  leading to the lambda coefficients  $\lambda^{SS}$  and  $\lambda^{BS}$  which are shown in figure 6.

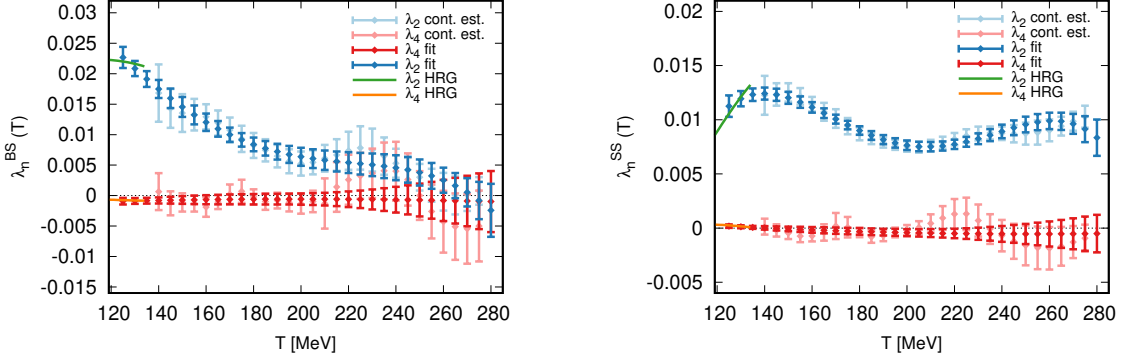


**Figure 6:** (Ref. [7]) Results of the shift analysis for  $\chi_2^S$  and  $\frac{\mu_S}{\mu_B}$ .

Let us denote the value of the dimensionless strange quark chemical potential that solves  $\chi_1^S = 0$  at fixed  $T$  and  $\hat{\mu}_B$  as  $\hat{\mu}_S^*$ . Still considering a fixed  $\hat{\mu}_B$  and  $T$ , but changing  $\hat{\mu}_S$  slightly from the strangeness neutral choice by a small amount:

$$\Delta\hat{\mu}_S \equiv \hat{\mu}_S - \hat{\mu}_S^*, \quad (5)$$

the dimensionless strangeness and baryon densities become:

$$\chi_1^S(\hat{\mu}_S) \approx \chi_2^S(\hat{\mu}_S^*)\Delta\hat{\mu}_S \quad (6)$$

$$\chi_1^B(\hat{\mu}_S) \approx \chi_1^B(\hat{\mu}_S^*) + \chi_{11}^{BS}(\hat{\mu}_S^*)\Delta\hat{\mu}_S, \quad (7)$$

where we only kept the linear leading order terms in  $\Delta\hat{\mu}_S$ . Now, we will express thermodynamic quantities in terms of the strangeness-to-baryon fraction:

$$R = \frac{\chi_1^S}{\chi_1^B} = \frac{\chi_2^S(\hat{\mu}_S^*)\Delta\hat{\mu}_S}{\chi_1^B(\hat{\mu}_S^*)\Delta\hat{\mu}_S + \chi_{11}^{BS}(\hat{\mu}_S^*)}. \quad (8)$$

Inverting this equation we get:

$$\Delta\hat{\mu}_S = \frac{R\hat{\chi}_1^B(\hat{\mu}_S^*)}{\chi_2^S(\hat{\mu}_S^*) - R\chi_{11}^{BS}(\hat{\mu}_S^*)}. \quad (9)$$

This quantity is shown for  $\hat{\mu}_B = 2$  as a function of temperature for various values of  $R$  in figure 7.

Substituting Eq.(9) into Eq.(7) we obtain (to leading order in  $R$ ):

$$\frac{\chi_1^B(T, \hat{\mu}_B, R)}{\chi_1^B(T, \hat{\mu}_B, R=0)} \approx 1 + R \frac{\chi_{11}^{BS}(T, \hat{\mu}_B, R=0)}{\chi_2^S(T, \hat{\mu}_B, R=0)}, \quad (10)$$

where all quantities on the right hand side are along the strangeness neutral line. We show the results of a leading order (in  $R$ ) extrapolation of the dimensionless baryon density as a function of  $T$  at  $\hat{\mu}_B = 2$  for several values of  $R$  in the left hand side of figure 8.

At the strangeness neutral line the  $O(R)$  correction of the pressure vanishes. The leading order correction gives:

$$\hat{p}(T, \hat{\mu}_B, R) \approx \hat{p}(T, \hat{\mu}_B, R=0) + \frac{1}{2} \frac{d^2 \hat{p}}{dR^2}(T, \hat{\mu}_B) R^2, \quad (11)$$

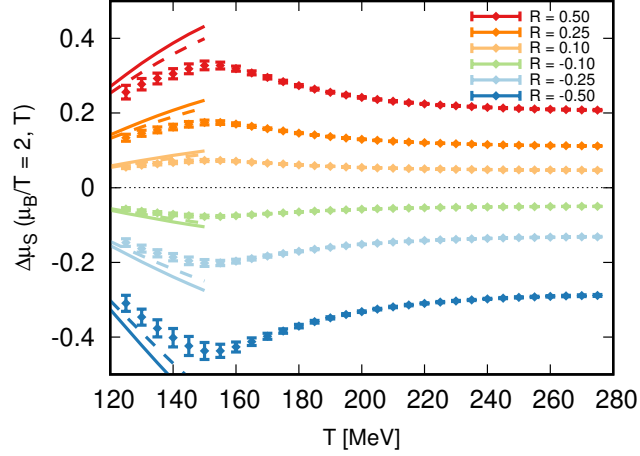


**Figure 7:** (Ref. [7]) Shift of the strangeness chemical potential as a function of the temperature at  $\hat{\mu}_B = 2$ , at various values of the strangeness-to-baryon ratio  $R = \chi_1^S / \chi_1^B$ . The solid lines show the exact solution of  $0.4\chi_1^B = \chi_1^S$  in the hadron resonance (HRG) model, while the dashed lines show the evaluation of the approximation of Eq. (9) in the HRG model.

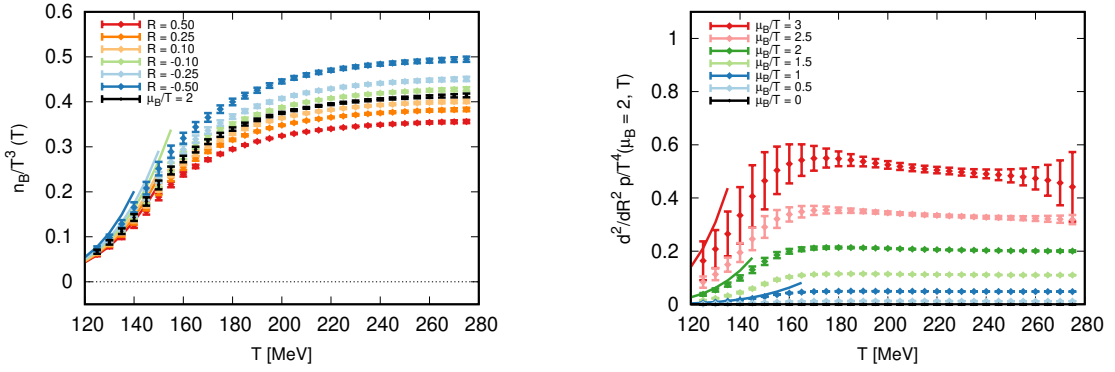


**Figure 8:** (Ref. [7]) Left: The dimensionless baryon density as a function of the temperature at  $\hat{\mu}_B = 2$ , for various values of the strangeness-to-baryon ratio  $R = \chi_1^S / \chi_1^B$ . Right: The leading order Taylor coefficient of the pressure in the strangeness-to-baryon ratio  $R$  on the strangeness neutral line as a function of the temperature for several fixed values of  $\hat{\mu}_B$ .

where

$$\frac{d^2 \hat{p}}{dR^2} = \frac{\chi_1^B(T, \hat{\mu}_B, R = 0)}{[\chi_2^S(T, \hat{\mu}_B, R = 0) - R\chi_{11}^{BS}(T, \hat{\mu}_B, R = 0)]^2}. \quad (12)$$

We show the results of a leading order (in  $R$ ) extrapolation of the dimensionless pressure as a function of  $T$  at  $\hat{\mu}_B = 2$  for several values of  $R$  in the right hand side of figure 8.

#### 4. Cross-check

In Ref. [16] we present a study of the equation of state of a quark gluon plasma at high temperatures and densities from direct lattice simulations by employing reweighting techniques. While large lattices as discussed throughout the rest of this proceedings are currently out of reach,

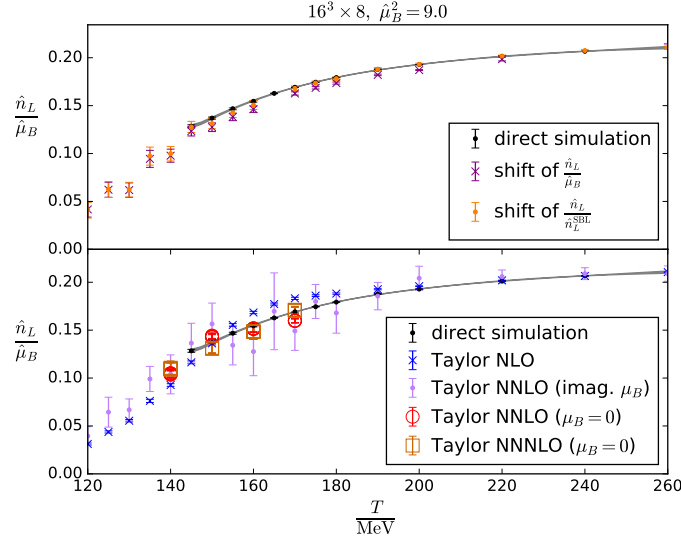


**Figure 9:** (Ref. [16]) Comparison of different extrapolation methods for  $\hat{n}_L$  as defined in equation (13) with direct simulations. The top panel shows the results of the resummation schemes without Stefan-Boltzmann correction (Ref. [14]) in violet and with Stefan-Boltzmann correction (Ref. [7]) in orange as discussed in this proceedings. The bottom panel shows the results from the Taylor expansion either directly from the  $\mu_B = 0$  data or from imaginary chemical potential. A spline interpolation of the direct results is included to lead the eye.

we can test several extrapolation techniques with high precision on a  $16^3 \times 8$  lattice with  $\mu_s = 0$  (leading to  $\mu_s = \frac{\mu_B}{3}$ ). We execute each analysis on this lattice ensemble and show the results in figure 9 for the observable

$$\hat{n}_L(T, \hat{\mu}_B) = \frac{d\hat{p}}{d\hat{\mu}_B} = \frac{1}{3(LT)^3} \left( \frac{\partial \ln Z(T, \hat{\mu}_B)}{\partial \hat{\mu}_q} \right)_{\mu_s=0}. \quad (13)$$

In the top panel we present the result for the resummation methods discussed in this proceedings. We compare the analysis from Ref. [14] without the Stefan-Boltzmann correction with the one from Ref. [7] where the correction is included. As expected the addition of the Stefan-Boltzmann correction allows the fast convergence at high temperatures and the extrapolated data agrees with the direct simulation within errors. In the bottom panel we compare Taylor expansion results to various order. We use two different methods to determine the Taylor expansion: On the one hand we compute it directly from the  $\mu_B = 0$  data. On the other hand we can use the imaginary  $\mu_B$  data to measure the Taylor coefficients. For this specific setup the later method results in considerably larger errors. We assume this is related to the small volume. The errors obtained when using the imaginary potential are too large for a valuable comparison. For the sufficiently small errors the Taylor extrapolation from  $\mu = 0$  agrees with the direct simulation if the NNNLO (up to  $\hat{\mu}_B^6$ ) term is included. This means that about one order more of the expansion is required than for the resummation method where the expansion agrees with the direct method if  $\lambda_4$  is included which only requires the  $\hat{\mu}_B^6$  term.

## Acknowledgments

The project was supported by the BMBF Grant No. 05P18PXFCA and 05P21PXFCA as well as the MKW NRW under the funding code NW21-024-A. This work was also supported by the Hungarian National Research, Development and Innovation Office, NKFIH grant KKP126769. This material is based upon work supported by the National Science Foundation under grants no. PHY-1654219, PHY-2208724, PHY-2116686 and OAC-2103680. A.P. is supported by the J. Bolyai Research Scholarship of the Hungarian Academy of Sciences and by the ÚNKP-21-5 New National Excellence Program of the Ministry for Innovation and Technology. The authors gratefully acknowledge the Gauss Centre for Supercomputing e.V. ([www.gauss-centre.eu](http://www.gauss-centre.eu)) for funding this project by providing computing time on the GCS Supercomputers HAWK at HLRS, Stuttgart as well as the JUWELS/Booster and JURECA/Booster at FZ-Juelich. Part of the computation was performed on the QPACE3 funded by the DFG and hosted by JSC.

## References

- [1] S. Borsanyi, G. Endrodi, Z. Fodor, A. Jakovac, S.D. Katz, S. Krieg et al., *The QCD equation of state with dynamical quarks*, *JHEP* **11** (2010) 077 [[1007.2580](#)].
- [2] S. Borsanyi, Z. Fodor, C. Hoelbling, S.D. Katz, S. Krieg and K.K. Szabo, *Full result for the QCD equation of state with 2+1 flavors*, *Phys. Lett. B* **730** (2014) 99 [[1309.5258](#)].
- [3] HotQCD collaboration, *Equation of state in (2+1)-flavor QCD*, *Phys. Rev. D* **90** (2014) 094503 [[1407.6387](#)].
- [4] K. Kajantie, M. Laine, K. Rummukainen and Y. Schroder, *The Pressure of hot QCD up to  $g_6 \ln(1/g)$* , *Phys. Rev. D* **67** (2003) 105008 [[hep-ph/0211321](#)].
- [5] J.O. Andersen, L.E. Leganger, M. Strickland and N. Su, *NNLO hard-thermal-loop thermodynamics for QCD*, *Phys. Lett. B* **696** (2011) 468 [[1009.4644](#)].
- [6] J.O. Andersen, L.E. Leganger, M. Strickland and N. Su, *Three-loop HTL QCD thermodynamics*, *JHEP* **08** (2011) 053 [[1103.2528](#)].
- [7] S. Borsanyi, J.N. Guenther, R. Kara, Z. Fodor, P. Parotto, A. Pasztor et al., *Resummed lattice QCD equation of state at finite baryon density: Strangeness neutrality and beyond*, *Phys. Rev. D* **105** (2022) 114504 [[2202.05574](#)].
- [8] R. Bellwied, S. Borsanyi, Z. Fodor, S.D. Katz, A. Pasztor, C. Ratti et al., *Fluctuations and correlations in high temperature QCD*, *Phys. Rev. D* **92** (2015) 114505 [[1507.04627](#)].
- [9] H.T. Ding, S. Mukherjee, H. Ohno, P. Petreczky and H.P. Schadler, *Diagonal and off-diagonal quark number susceptibilities at high temperatures*, *Phys. Rev. D* **92** (2015) 074043 [[1507.06637](#)].
- [10] A. Bazavov et al., *The QCD Equation of State to  $O(\mu_B^6)$  from Lattice QCD*, *Phys. Rev. D* **95** (2017) 054504 [[1701.04325](#)].

- [11] HotQCD collaboration, *Taylor expansions and Pade approximants for cumulants of conserved charge fluctuations at nonvanishing chemical potentials*, *Phys. Rev. D* **105** (2022) 074511 [2202.09184].
- [12] S. Borsanyi, Z. Fodor, J.N. Guenther, S.K. Katz, K.K. Szabo, A. Pasztor et al., *Higher order fluctuations and correlations of conserved charges from lattice QCD*, **1805.04445**.
- [13] A. Bazavov et al., *Skewness, kurtosis, and the fifth and sixth order cumulants of net baryon-number distributions from lattice QCD confront high-statistics STAR data*, *Phys. Rev. D* **101** (2020) 074502 [2001.08530].
- [14] S. Borsányi, Z. Fodor, J.N. Guenther, R. Kara, S.D. Katz, P. Parotto et al., *Lattice QCD equation of state at finite chemical potential from an alternative expansion scheme*, *Phys. Rev. Lett.* **126** (2021) 232001 [2102.06660].
- [15] S. Borsanyi, Z. Fodor, J.N. Guenther, R. Kara, S.D. Katz, P. Parotto et al., *The QCD crossover at finite chemical potential from lattice simulations*, **2002.02821**.
- [16] S. Borsanyi, Z. Fodor, M. Giordano, J.N. Guenther, S.D. Katz, A. Pasztor et al., *Equation of state of a hot-and-dense quark gluon plasma: lattice simulations at real  $\mu_B$  vs. extrapolations*, **2208.05398**.